Available online at www.sciencedirect.com
SCIENCE DIRECT®
ELSEVIER
International Journal of Solids and Structures 41 (2004) 6529–6547
INTERNATIONAL JOURNAL OF SOLIDS and STRUCTURES
www.elsevier.com/locate/ijsolstr

Higher-order free vibrations of sandwich beams with a locally damaged core

Vladimir S. Sokolinsky [a,*], Hubertus F. von Bremen [b], John J. Lesko [c], Steven R. Nutt [d]

[a] *Alpha STAR Corporation, 5199 East Pacific Coast Highway, Suite 410, Long Beach, CA 90804, USA*
[b] *Department of Mathematics, University of Southern California, Los Angeles, CA 90089-1113, USA*
[c] *Engineering Science and Mechanics Department, Virginia Tech, Blacksburg, VA 24061, USA*
[d] *Department of Materials Science, University of Southern California, Los Angeles, CA 90089-0241, USA*

Received 2 August 2003; received in revised form 24 May 2004
Available online 2 July 2004

Abstract

The dynamical equations describing the free vibration of sandwich beams with a locally damaged core are derived using the higher-order theory approach. The nonlinear acceleration fields in the core are accounted for in the derivations, which is essential for the vibration analysis of the locally damaged sandwich beams. A local damage in the core, arbitrarily located along the length of the sandwich beam, is assumed to preclude the transition of stresses through the core between the undamaged parts of the beam. The damage is assumed to exist before the vibration starts and not to grow during oscillations. The numerical analysis based on the derived equations has been verified with the aid of the commercial finite element software ABAQUS. The numerical simulations reveal that a small local damage causes significant changes in the natural frequencies and corresponding vibration modes of the sandwich beams. An important practical consequence of the present work is that the vibration measurements can be successfully used as a nondestructive damage tool to assess local damages in sandwich beams.

Keywords: Sandwich beam; Locally damaged core; Higher-order approach; Vibrations; Natural frequencies; FEM validation

1. Introduction

The idea of investigating the change in the natural vibration frequencies as an indicator of damage in composite structures is not new. Kulkarni and Frederick (1971) suggested that the natural frequency of a circular cylindrical shell reflected the presence of delamination in the composite layout. Cawley and Adams (1979) went further and pointed out that the shift in natural frequencies due to delamination in fiber composite structures provided a basis for nondestructive testing techniques.

* Corresponding author. Tel.: +1-5629851100x35; fax: +1-5629850786.
E-mail address: vsokolinsky@alphastarcorp.com (V.S. Sokolinsky).

0020-7683/$ - see front matter © 2004 Elsevier Ltd. All rights reserved.
doi:10.1016/j.ijsolstr.2004.05.059

The interpretation of such observations used in the detection of damage in sandwich structures requires development of an accurate vibration theory. An analytical approach to the free vibration response of debonded sandwich beams with a honeycomb core was reported in the work of Hu and Hwu (1995). In their analysis, the beam is divided into four parts, and the core displacements in each region are treated as Timoshenko beam elements. The influence of geometric and material parameters of the core and face sheets were explored. In addition, the effects of debonding length on the natural frequencies and associated mode shapes of the delaminated honeycomb sandwich beam were investigated. In related work of Kim and Hwang (2002), the split beam model was used in conjunction with classical sandwich theory to analyze the effect of debonding on the natural frequencies and frequency response functions, as well as on the flexural rigidity of honeycomb sandwich beams. The results of the study showed that debonding reduces the natural frequencies of honeycomb sandwich beams.

The aim of the present paper is to investigate the free vibration behavior of sandwich beams with a locally damaged transversely flexible (soft) core for which the ratio of the Young's moduli of the isotropic face sheets to the core lies between 500 and 1000. Higher-order theory assumptions (Frostig, 1992) and a consistent dynamic approach (Sokolinsky and Nutt, 2004) are used to derive the free vibration equations for the sandwich beams with a locally damaged soft core. The numerical approach used to discretize the partial differential equations with associated boundary and continuity conditions consists of the harmonic motion assumption and the direct finite difference method. The numerical analysis based on the derived equations has been verified with the aid of the commercial finite element software ABAQUS. The numerical results demonstrate that a local damage of small length, which is located in the span of a soft-core sandwich beam, leads to significant reduction in the natural frequencies and their corresponding vibration modes. These findings could provide the foundation for the development of vibration-based nondestructive evaluation techniques and health monitoring approaches.

2. Mathematical formulation

2.1. Analytical model

The free vibration equations for sandwich beams with isotropic face sheets and a locally damaged transversely flexible (soft) core are derived using the higher-order theory of sandwich panels (Frostig, 1992). In the higher-order theory, the face sheets of the sandwich beams are treated as ordinary beams with negligible shear strains that follow Euler–Bernoulli assumptions, and are subject to small deformations. The soft core is treated as a two-dimensional elastic medium with small deformations where the height may change under loading, and the cross-section does not remain planar. The longitudinal (in-plane) stresses in the core in the undamaged regions are neglected because the core material possesses a significantly lower modulus than the face sheets. Both experimental and analytical studies (Thomsen and Frostig, 1997; Swanson and Kim, 2000) have clearly demonstrated the justification for the neglect of the in-plane stresses in the soft core. The interface layers between the face sheets and the core at the undamaged regions are assumed to be rigid and provide continuity of the deformations at the core-face sheet interface.

In the present model, a small local damage in the core, which is arbitrarily located along the length of the sandwich beam, is assumed to preclude the transition of stresses through the core between the undamaged parts of the beam. This assumption is reasonable because an impact on the face sheet may significantly impair the ability of the core material to transfer the stresses through the small damaged region. The damage is assumed to exist *prior* to vibration and to be constant in length during the oscillations (see Fig. 1).

Therefore, the longitudinal (σ_{xx}) and vertical normal stresses (σ_{zz}) and the shear stress (τ) in the core through the small damaged region are assumed to be zero (see Fig. 2).

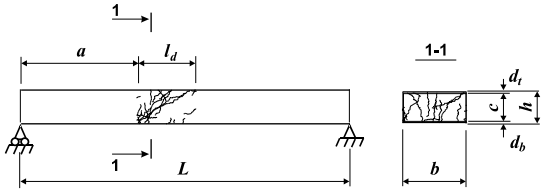

Fig. 1. Schematic of the locally damaged sandwich beam.

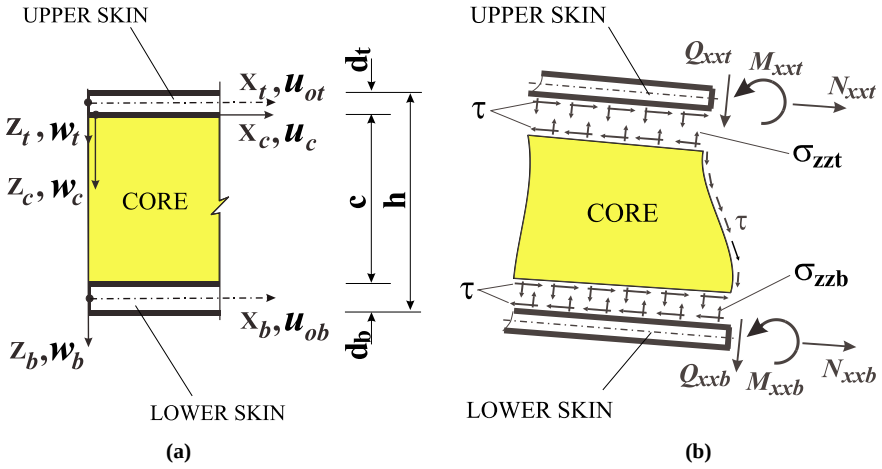

Fig. 2. Geometry (a) and internal resultants (b) of a sandwich beam.

The acceleration fields of the face sheets and the core are assumed to have the same shape as the corresponding static deformation fields (Sokolinsky and Nutt, 2004). Namely, the acceleration fields of the face sheets vary linearly with height, whereas the acceleration fields of the core in the longitudinal and vertical directions vary *nonlinearly* with height.

Accounting for the nonlinear acceleration fields in the core is essential for analysis of the free vibration response of sandwich beams with a locally damaged core. Unlike an undamaged structure, the inertia loads exerted on the damaged sandwich beams are *not* uniformly distributed along the span.

2.2. Equations of motion

A local damage between the upper face sheet and the core divides a sandwich beam into three regions—two undamaged and one damaged (see Fig. 1). The kinematic assumptions for the upper ($i = t$) and lower ($i = b$) face sheets for all regions read

$$u_i(x_i, t) = u_{0i}(x_i, t) - z_i w_{i,x}(x_i, t) \tag{1}$$

where x_i, y_i, z_i are the local rectangular coordinates of the upper and lower face sheets, $u_i(x_i, t)$ and $w_i(x_i, t)$ are the longitudinal and vertical displacements, respectively, for any point on the cross-section of the upper and lower face sheets, $u_{0i}(x_i, t)$ are the longitudinal displacements of the centroid lines of the upper and lower face sheets, and t is a time coordinate (see Fig. 2(a)).

The kinematic assumptions for the horizontal and vertical displacements of a soft core at the undamaged region are given, respectively, by

$$u_c(x_c,t) = (z_c/G_c)\tau(x_c,t) - (z_c^2 c/2 - z_c^3/3)(2E_c)\tau_{,xx}(x_c,t) - (z_c^2/2c)w_{b,x}(x_c,t) - (-z_c^2/2c + z_c + d_t/2)w_{t,x}(x_c,t) + u_{0t}(x_c,t) \tag{2}$$

$$w_c(x_c,t) = z_c(c - z_c)/(2E_c)\tau_{,x}(x_c,t) + (1 - z_c/c)w_t(x_c,t) + (z_c/c)w_b(x_c,t) \tag{3}$$

where x_c, y_c, z_c are the local rectangular coordinates of the core, τ is the shear stress in the core, E_c and G_c are the Young's and the shear moduli of the core, respectively, c is the height of the core, and d_t is the thickness of the upper face sheet (see Fig. 2(a)).

At the damaged region—assuming detachment of the core material from the upper face sheet as the result of impact the—horizontal and vertical displacements of the core are

$$u_c(x_c,t) = u_{0b}(x_b,t) + (d_b/2)w_{b,x}(x_b,t) \tag{4}$$

$$w_c(x_c,t) = w_b(x_b,t) \tag{5}$$

where d_b is the thickness of the lower face sheet (see Fig. 2(a)).

The foregoing kinematic relations are used for the derivation of the Lagrangian for a sandwich beam.

In what follows, Hamilton's variational principle is applied to derive the partial differential equations describing the linear free vibrations of the sandwich beams with a locally damaged soft core for both undamaged and damaged regions, the continuity requirements connecting the damaged and undamaged regions together, and the boundary conditions at the edges of the sandwich beam. The equation is

$$\int_{t_1}^{t_2} \delta L \, dt = 0, \quad \delta \mathbf{v}(t_1) = \delta \mathbf{v}(t_2) = 0 \tag{6}$$

where L is the Lagrangian, $\mathbf{v}$ is the vector of unknowns describing the deformed state of a sandwich beam between the time instants t_1 and t_2 and δ represents the variation.

The strain and kinetic energy of the isotropic face sheets for both the undamaged and damaged region, respectively, read

$$V_F = \frac{1}{2}\int_{L_j} (EA_t u_{0t,x}^2 + EI_t w_{t,xx}^2 + EA_b u_{0b,x}^2 + EI_b w_{b,xx}^2)\, dx \tag{7}$$

$$T_F = \frac{1}{2}\int_{L_j} \left\{ [\rho_t A_t(\dot{u}_{0t}^2 + \dot{w}_t^2) + \rho_t I_t \dot{w}_{t,x}^2] + [\rho_b A_b(\dot{u}_{0b}^2 + \dot{w}_b^2) + \rho_b I_b \dot{w}_{b,x}^2] \right\} dx \tag{8}$$

where EA_i are the axial rigidities of the upper ($i = t$) and lower ($i = b$) face sheets, EI_i are the flexural rigidities of the face sheets, ρ_i are the mass densities of the face sheets, A_t and A_b and I_t and I_b are the cross-sectional areas and the area moments of inertia of the upper and lower face sheets, respectively, and L_j denotes the undamaged ($j = u$) and the damaged ($j = d$) parts of the sandwich beam.

In the undamaged region, the strain and kinetic energy of the isotropic transversely flexible core, using the nonlinear displacement fields in Eqs. (2) and (3), are given by

$$V_C^u = \frac{1}{2}\int_{L_u} b\left[\frac{c}{G_c}\tau^2 + \frac{c^3}{12E_c}\tau_{,x}^2 + \frac{E_c}{c}(w_t^2 + w_b^2 - 2w_t w_b)\right] dx \tag{9}$$

$$
\begin{aligned}
T_C^u = \frac{1}{2}\int_{L_u} b\rho_c \Big\{ & (c^3/3G_c^2)\dot{\tau}^2 + (13c^7/5040E_c^2)\dot{\tau}_{,xx}^2 + (c^3/20)\dot{w}_{b,x}^2 \\
& + [(2/15)c^3 + (d_t/3)c^2 + (d_t^2/4)c]\dot{w}_{t,x}^2 + c\dot{u}_{0t}^2 - (7c^5/120E_cG_c)\dot{\tau}\dot{\tau}_{,xx} \\
& - (c^3/4G_c)\dot{\tau}\dot{w}_{b,x} - [2(5c^3/24 + c^2d_t/4)/G_c]\dot{\tau}\dot{w}_{t,x} + (c^2/G_c)\dot{\tau}\dot{u}_{0t} \\
& + (c^5/45E_c)\dot{\tau}_{,xx}\dot{w}_{b,x} + [(13c^5/360 + c^4d_t/24)E_c]\dot{\tau}_{,xx}\dot{w}_{t,x} \\
& - (c^4/12E_c)\dot{\tau}_{,xx}\dot{u}_{0t} + (3c^3/20 + c^2d_t/6)\dot{w}_{b,x}\dot{w}_{t,x} - (c^2/3)\dot{w}_{b,x}\dot{u}_{0t} \\
& - (2c^2/3 + d_tc)\dot{w}_{t,x}\dot{u}_{0t} + (c^5/120E_c^2)\dot{\tau}_{,x}^2 + (c/3)\dot{w}_t^2 + (c/3)\dot{w}_b^2 + (c^3/12E_c)\dot{\tau}_{,x}\dot{w}_t \\
& + (c^3/12E_c)\dot{\tau}_{,x}\dot{w}_b + (c/3)\dot{w}_t\dot{w}_b \Big\} \mathrm{d}x
\end{aligned} \tag{10}
$$

where b is the width of the sandwich beam (see Fig. 1).

Because the shear, τ, and horizontal, σ_{xx}, and vertical, σ_{zz}, normal stresses in the core are assumed to be zero throughout the damaged region (see Fig. 2(b)), the strain energy of the core is zero at the damaged part of the sandwich beam. The kinetic energy of the isotropic core in the damaged region is

$$
T_C^d = \frac{1}{2}\int_{L_d} A_c\rho_c \left\{ \dot{u}_{0b}^2 + d_b\dot{u}_{0b}\dot{w}_{b,x} + \frac{1}{4}d_b^2\dot{w}_{b,x}^2 + \dot{w}_b^2 \right\} \mathrm{d}x \tag{11}
$$

where A_c and ρ_c are the cross-sectional area and the mass density of the core, respectively.

Eqs. (2) and (3) assure the vertical compatibility at both interfaces and the longitudinal compatibility only at the upper interface layer. To ensure compatibility between the lower face sheet and the core in the longitudinal direction through the undamaged region, the following condition must be added to the Hamilton's principle in Eq. (6):

$$
u_c(x_c, z_c = c, t) = u_{0b}(x_b, t) + \frac{d_b}{2}w_{b,x}(x_b, t) \tag{12}
$$

which, after the use of Eq. (2) and multiplication by b yields the following auxiliary condition for the undamaged region:

$$
bu_{0b} - bu_{0t} - (bc/G_c)\tau + (bc^3/12E_c)\tau_{,xx} + [b(c + d_t)/2]w_{t,x} + [b(c + d_b)/2]w_{b,x} = 0 \tag{13}
$$

The free vibration equations for the undamaged region of a sandwich beam are derived through the constrained variation of Eq. (6) using the Lagrangian multiplier method (Lanczos, 1997; Lopez, 2001). The Lagrange multiplier can be shown to be the shear stress,τ, in the core that permits representation of the higher-order formulation in terms of the vector $\mathbf{v}(x, t) = \{u_{0b}, u_{0t}, w_b, w_t, \tau\}$. Thus, for the undamaged region, the free vibration equations for sandwich beams with a soft isotropic core and isotropic face sheets, which take into consideration the nonlinear acceleration fields in the core, are

$$
\begin{aligned}
& EA_tu_{0t,xx} + b\tau - \rho_tA_t\ddot{u}_{0t} - \rho_cA_c\left[\frac{13}{35}\ddot{u}_{0t} + \frac{9}{70}\ddot{u}_{0b} - \frac{1}{210}(11c + 39d_t)\ddot{w}_{t,x}\right. \\
& \quad \left. + \frac{1}{420}(13c + 27d_b)\ddot{w}_{b,x} + \frac{3}{140}(c/G_c)\ddot{\tau}\right] = 0
\end{aligned} \tag{14}
$$

$$
\begin{aligned}
& EA_bu_{0b,xx} - b\tau - \rho_bA_b\ddot{u}_{0b} - \rho_cA_c\left[\frac{9}{70}\ddot{u}_{0t} + \frac{13}{35}\ddot{u}_{0b} - \frac{1}{420}(13c + 27d_t)\ddot{w}_{t,x}\right. \\
& \quad \left. + \frac{1}{210}(11c + 39d_b)\ddot{w}_{b,x} - \frac{3}{140}(c/G_c)\ddot{\tau}\right] = 0
\end{aligned} \tag{15}
$$

$$EI_t w_{t,xxxx} + (bE_c/c)(w_t - w_b) - \frac{1}{2}b(c+d_t)\tau_{,x} + \rho_t A_t \ddot{w}_t - \rho_t I_t \ddot{w}_{t,xx} + \rho_c A_c \left\{ \frac{1}{210}(11c+39d_t)\ddot{u}_{0t,x} + \frac{1}{420}(13c+27d_t)\ddot{u}_{0b,x} + \frac{1}{3}\ddot{w}_t - \frac{1}{420}(4c^2+22cd_t+39d_t^2)\ddot{w}_{t,xx} + \frac{1}{6}\ddot{w}_b + \frac{1}{840}[6c^2+13c(d_t+d_b)+27d_td_b]\ddot{w}_{b,xx} + \frac{1}{840}(c/E_cG_c)[35cG_c+E_c(2c+9d_t)]\ddot{\tau}_{,x} \right\} = 0 \tag{16}$$

$$EI_b w_{b,xxxx} - (bE_c/c)(w_t - w_b) - \frac{1}{2}b(c+d_b)\tau_{,x} + \rho_b A_b \ddot{w}_b - \rho_b I_b \ddot{w}_{b,xx} - \rho_c A_c \left\{ \frac{1}{420}(13c+27d_b)\ddot{u}_{0t,x} + \frac{1}{210}(11c+39d_b)\ddot{u}_{0b,x} - \frac{1}{6}\ddot{w}_t - \frac{1}{840}(6c^2+13c(d_t+d_b)+27d_td_b)\ddot{w}_{t,xx} - \frac{1}{3}\ddot{w}_b + \frac{1}{420}[4c^2+22cd_b+39d_b^2]\ddot{w}_{b,xx} - \frac{1}{840}(c/E_cG_c)[35cG_c+E_c(2c+9d_b)]\ddot{\tau}_{,x} \right\} = 0 \tag{17}$$

$$bu_{0t} - bu_{0b} - [b(c+d_t)/2]w_{t,x} - [b(c+d_b/2]w_{b,x} - (bc^3/12E_c)\tau_{,xx} + (bc/G_c)\tau + (A_c\rho_c c/E_cG_c)\left\{ \frac{1}{140}(14G_c-3E_c)(\ddot{u}_{0t}-\ddot{u}_{0b}) - \frac{1}{840}[G_c(7c+42d_t)-E_c(2c+9d_t)]\ddot{w}_{t,x} - \frac{1}{840}[G_c(7c+42d_b)-E_c(2c+9d_b)]\ddot{w}_{b,x} + \frac{1}{210}(c/G_c)[21G_c-E_c]\ddot{\tau} \right\} = 0 \tag{18}$$

Notice that the effect of the rotatory inertia (Shames and Dym, 1985) of the face sheets is accounted for in the governing equations stated above.

Eqs. (14) and (15) represent dynamic equilibrium in the horizontal direction and Eqs. (16) and (17) in the vertical direction of the upper and lower face sheets supported by a soft core. Furthermore, Eq. (18) is a combination of the compatibility condition in the longitudinal direction at the lower interface layer (see Eq. (13)) and the dynamic terms. As follows from the variational procedure, these dynamic terms add to zero, which implies the proper fulfillment of the compatibility at the lower interface in the present formulation. Retention of the dynamic terms in Eq. (18) provides structural uniformity of all the dynamic equilibrium equations for the undamaged region (Eqs. (14)–(18)). Namely, as anticipated on physical grounds, each dynamic equation is comprised of elastic and dynamic contributions, which mathematically leads to *consistency* between the ranks of stiffness and mass matrix differential operators.

For the damaged region, the free vibration equations appear as

$$EA_t u_{0t,xx} - \rho_t A_t \ddot{u}_{0t} = 0 \tag{19}$$

$$EA_b u_{0b,xx} - (\rho_b A_b + \rho_c A_c)\ddot{u}_{0b} - (1/2)\rho_c A_c d_b \ddot{w}_{b,x} = 0 \tag{20}$$

$$EI_t w_{t,xxxx} + \rho_t A_t \ddot{w}_t - \rho_t I_t \ddot{w}_{t,xx} = 0 \tag{21}$$

$$EI_b w_{b,xxxx} + (\rho_b A_b + \rho_c A_c)\ddot{w}_b - (\rho_b I_b + \rho_c A_c d_b^2/4)\ddot{w}_{b,xx} - (1/2)\rho_c A_c d_b \ddot{u}_{0b,x} = 0 \tag{22}$$

Because the shear stress in the core, τ, in the damaged region equals zero, only four dynamic equilibrium equations are required to calculate the remaining unknown functions (u_{0b}, u_{0t}, w_b, w_t). In this case, compatibility at the upper interface is assumed to not exist through the damaged region as the result of impact, whereas at the lower interface, compatibility between the lower face sheet and the core is given by Eqs. (4) and (5).

The continuity requirements between the undamaged and damaged regions at the left ($x = a$) and right ends ($x = a + l_d$) of the local damage are derived from the boundary terms, which result from the integration by parts through the undamaged (L_u) and damaged (L_d) regions. The kinematic conditions, which express the compatibility between the left (l) and right (r) sides of the cross-section of the upper and lower face sheets at the ends of the local damage are

$$u_{0t}^{(l)} = u_{0t}^{(r)} \tag{23}$$

$$u_{0b}^{(l)} = u_{0b}^{(r)} \tag{24}$$

$$w_t^{(l)} = w_t^{(r)} \tag{25}$$

$$w_b^{(l)} = w_b^{(r)} \tag{26}$$

$$w_{t,x}^{(l)} = w_{t,x}^{(r)} \tag{27}$$

$$w_{b,x}^{(l)} = w_{b,x}^{(r)} \tag{28}$$

Moreover, the natural continuity conditions for the face sheets at the ends of the damage read

$$u_{0t,x}^{(l)} - u_{0t,x}^{(r)} = 0 \tag{29}$$

$$u_{0b,x}^{(l)} - u_{0b,x}^{(r)} = 0 \tag{30}$$

$$w_{t,xx}^{(l)} - w_{t,xx}^{(r)} = 0 \tag{31}$$

$$w_{b,xx}^{(l)} - w_{b,xx}^{(r)} = 0 \tag{32}$$

$$\begin{aligned} &EI_t(w_{t,xxx}^{(l)} - w_{t,xxx}^{(r)}) - \frac{1}{2}bd_t\tau^{(\varsigma)} - \rho_t I_t(\ddot{w}_{t,x}^{(l)} - \ddot{w}_{t,x}^{(r)}) \\ &\quad + \rho_c A_c\left\{\frac{1}{210}(11c + 39d_t)\ddot{u}_{0t}^{(l)} + \frac{1}{420}(13c + 27d_t)\ddot{u}_{0b}^{(l)}\right. \\ &\quad - \frac{1}{420}(4c^2 + 22cd_t + 39d_t^2)\ddot{w}_{t,x}^{(l)} + \frac{1}{840}[6c^2 + 13c(d_t + d_b) + 27d_td_b]\ddot{w}_{b,x}^{(l)} \\ &\quad \left. + \frac{1}{840}(c/G_c)(2c + 9d_t)\ddot{\tau}^{(\varsigma)}\right\} = 0 \end{aligned} \tag{33}$$

$$\begin{aligned} &EI_b(w_{b,xxx}^{(l)} - w_{b,xxx}^{(r)}) - \frac{1}{2}bd_b\tau^{(\varsigma)} - \rho_b I_b(\ddot{w}_{b,x}^{(l)} - \ddot{w}_{b,x}^{(r)}) \\ &\quad - \rho_c A_c\left\{\frac{1}{420}(13c + 27d_b)\ddot{u}_{0t}^{(l)} + \frac{1}{210}(11c + 39d_b)\ddot{u}_{0b}^{(l)} - \frac{1}{2}d_b\ddot{u}_{0b}^{(r)}\right. \\ &\quad - \frac{1}{840}[6c^2 + 13c(d_t + d_b) + 27d_td_b]\ddot{w}_{t,x}^{(l)} + \frac{1}{420}(4c^2 + 22cd_b + 39d_b^2)\ddot{w}_{b,x}^{(l)} - \frac{1}{4}d_b^2\ddot{w}_{b,x}^{(r)} \\ &\quad \left. - \frac{1}{840}(c/G_c)(2c + 9d_b)\ddot{\tau}^{(\varsigma)}\right\} = 0 \end{aligned} \tag{34}$$

where $\varsigma = l$ at $x = a$ and $\varsigma = r$ at $x = a + l_d$.

The condition for the shear stress in the core through its height at the ends of the damaged region is

$$\tau^{(\varsigma)} = 0 \tag{35}$$

The boundary conditions at the undamaged edges of the sandwich beam ($x = 0, L$) are, for the upper face sheet,

$$EA_t u_{0t,x} = 0 \quad \text{or } u_{0t} \text{ is prescribed} \tag{36}$$

$$EI_t w_{t,xx} = 0 \quad \text{or } w_{t,x} \text{ is prescribed} \tag{37}$$

$$\begin{aligned} &- EI_t w_{t,xxx} + \frac{1}{2} b d_t \tau + \rho_t I_t \ddot{w}_{t,x} - \rho_c A_c \left\{ \frac{1}{210}(11c + 39d_t)\ddot{u}_{0t} + \frac{1}{420}(13c + 27d_t)\ddot{u}_{0b} \right. \\ &- \frac{1}{420}(4c^2 + 22cd_t + 39d_t^2)\ddot{w}_{t,x} + \frac{1}{840}[6c^2 + 13c(d_t + d_b) + 27d_t d_b]\ddot{w}_{b,x} \\ &\left. + \frac{1}{840}(c/G_c)(2c + 9d_t)\ddot{\tau} \right\} = 0 \quad \text{or } w_t \text{ is prescribed} \end{aligned} \tag{38}$$

for the lower face sheet,

$$EA_b u_{0b,x} = 0 \quad \text{or } u_{0b} \text{ is prescribed} \tag{39}$$

$$EI_b w_{b,xx} = 0 \quad \text{or } w_{b,x} \text{ is prescribed} \tag{40}$$

$$\begin{aligned} &- EI_b w_{b,xxx} + \frac{1}{2} b d_b \tau + \rho_b I_b \ddot{w}_{b,x} + \rho_c A_c \left\{ \frac{1}{420}(13c + 27d_b)\ddot{u}_{0t} + \frac{1}{210}(11c + 39d_b)\ddot{u}_{0b} \right. \\ &- \frac{1}{840}[6c^2 + 13c(d_t + d_b) + 27d_t d_b]\ddot{w}_{t,x} + \frac{1}{420}(4c^2 + 22cd_b + 39d_b^2)\ddot{w}_{b,x} \\ &\left. - \frac{1}{840}(c/G_c)(2c + 9d_b)\ddot{\tau} \right\} = 0 \quad \text{or } w_b \text{ is prescribed} \end{aligned} \tag{41}$$

and for the core through its height,

$$\tau = 0 \quad \text{or } \tau_{,x} \text{ is prescribed} \tag{42}$$

In the case of the damaged edge, namely, when $a = 0$ or $a = L - l_d$ (see Fig. 1), the following changes in the equations describing the boundary conditions at the undamaged edge (Eqs. (36)–(42)) are made. The boundary condition in the vertical direction at the upper face sheet (Eq. (38)) is changed to

$$-EI_t w_{t,xxx} + \rho_t I_t \ddot{w}_{t,x} = 0 \quad \text{or } w_t \text{ is prescribed} \tag{43}$$

whereas the boundary condition in the vertical direction at the lower face sheet (Eq. (41)) is replaced with

$$-EI_b w_{b,xxx} + \rho_b I_b \ddot{w}_{b,x} + \frac{1}{2}\rho_c A_c d_b \left\{ \ddot{u}_{0b} + \frac{1}{2} d_b \ddot{w}_{b,x} \right\} = 0 \quad \text{or } w_b \text{ is prescribed} \tag{44}$$

Finally, the boundary condition at the core edge (Eq. (42)) is omitted because the value of the shear stress is known to be equal to zero at the damaged edge.

Thus, through the derived formulation, the actual two-dimensional problem in space is mathematically treated as one-dimensional, which is of vital importance for the efficiency of numerical analysis (see Section 5).

3. Numerical analysis

The discretization of the equations of motion presented above is achieved using the harmonic motion assumption and the direct finite difference approach. The free vibration response of a locally damaged sandwich beam in terms of the main unknown functions can be represented as

$$\mathbf{v}(x,t) = \mathbf{v}(x)\mathrm{e}^{\mathrm{i}\omega t} \tag{45}$$

where $\mathbf{v}(x)$ is the 5×1 vector of the one-dimensional unknowns $\bar{u}_{0b}(x)$, $\bar{u}_{0t}(x)$, $\bar{w}_b(x)$, $\bar{w}_t(x)$, and $\bar{\tau}(x)$. A central difference scheme with fictitious grid points at the boundaries is applied so that the equations of motion are also satisfied at the beam edges. Moreover, the highest order of the derivatives in the continuous formulation is reduced to two through the introduction of the new functions

$$\hat{w}_t(x) = \bar{w}_{t,xx}(x) \quad \text{and} \quad \hat{w}_b(x) = \bar{w}_{b,xx}(x) \tag{46}$$

The generalized eigenvalue problem with the large sparse matrices of the general type is efficiently solved using the deflated iterative Arnoldi algorithm (Saad, 1992). The analysis outlined above has been implemented in dynamic modules of the computer code "FSAN" developed with the aid of the symbolic mathematical software "Maple" (Heal et al., 2000) running in the "MATLAB" (The MathWorks, 2001) software environment.

4. Results and discussion

In this section, the higher-order numerical analysis of sandwich beams with a locally damaged core is applied to the layouts widely used in measurements of the natural frequencies of sandwich beams. Namely, a cantilever (Fig. 3(a)) and a simply supported sandwich beam layout (Fig. 6(a)) are considered. The numerical simulations based on the derived equations reveal that the small local damages in the soft core cause significant change in the natural frequencies and corresponding vibration modes of the soft-core sandwich beams.

In the following simulations, the mechanical properties of the face sheets correspond to a quasi-isotropic material of density 4400 kg/m^3, whereas those of the core correspond to isotropic polymethacrylimide rigid foam of density $\sim$52 kg/m^3. The Poisson's ratios of the face sheets and core are 0.30 and 0.25, respectively.

4.1. Cantilever beam

Natural mode shapes of a cantilever sandwich beam with a local damage centered at the midspan (Fig. 3(a)) are presented in Fig. 3(b). As shown in the figure, the mode shapes of the structure with a locally damaged core differ significantly from those of the ordinary (undamaged) cantilever sandwich beam. Because the uniform distribution of inertia forces through the span characteristic of ordinary sandwich beams is violated, the mode shape *cannot* be described by a harmonic function of the longitudinal coordinate.

Comparison of the natural frequencies of Fig. 3(b) with those of the ordinary cantilever sandwich beam (see Sokolinsky et al., 2002) reveals that a midspan local damage with a length of only $\sim$3% of the beam span causes a reduction in the third natural frequency of $\sim$32% (see Table 1). Notice, in particular, that sandwich structures typically consist of face sheets that are much thinner than the core. For such thin face sheets, flexural stiffness is very small. Consequently, the clamping effect is manifest only in close proximity to the clamped end. This distance is negligible compared with the beam span, making it impractical to portray a zero slope that could be discerned by the reader.

Deeper insight into the free vibration response of a damaged sandwich cantilever in Fig. 3 can be gained by studying the dependence of its natural frequencies on the location of a local damage along the span of

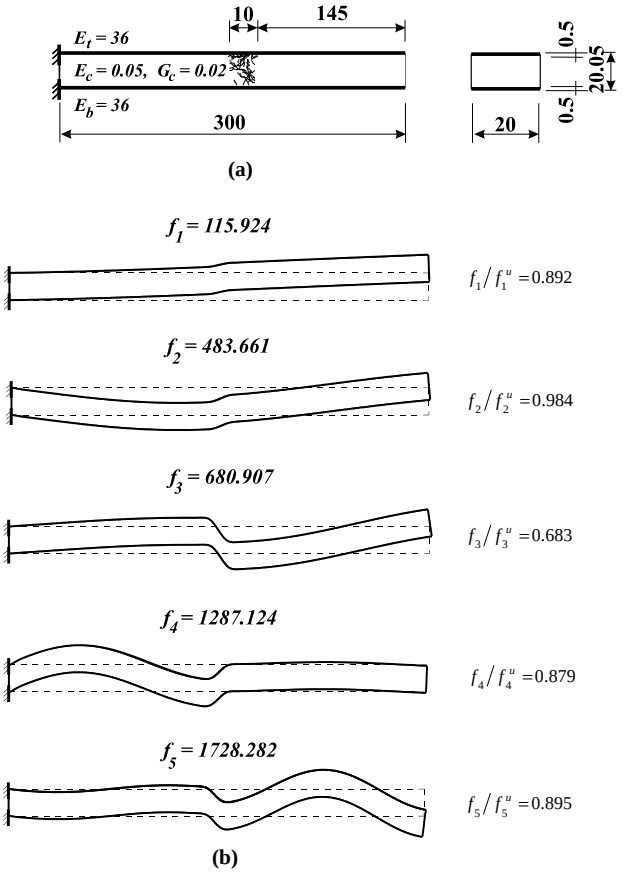

Fig. 3. Cantilever sandwich beam with local damage centered at midspan: (a) layout; (b) natural vibration modes and corresponding frequencies (Hertz) (dimensions in millimeters; moduli in gigapascal).

Table 1
Comparison of the natural frequencies of the cantilever sandwich beam

	Natural frequency (Hz)				
	1	2	3	4	5
Ordinary, f_n^u	130.0	491.4	996.3	1465.1	1930.7
Damaged, f_n	115.9	483.7	680.9	1287.1	1728.3
Difference, %	−10.8	−1.6	−31.7	−12.1	−10.5

the beam. The dependence of the fundamental frequency, and of the third natural frequency of the sandwich cantilever in Fig. 3(a) at the site of the 10 mm local damage along the span is shown in Fig. 4(a) and (b), respectively. In Fig. 4, the ratio of the particular frequency of the damaged sandwich beam to the corresponding frequency of the ordinary beam (marked by the superscript "u") (see Table 1) is shown along the vertical axis. The relative location of the local damage in the span is shown along the horizontal axis, where a stands for the distance from the left edge of a damage to the left edge of the beam (see Fig. 1).

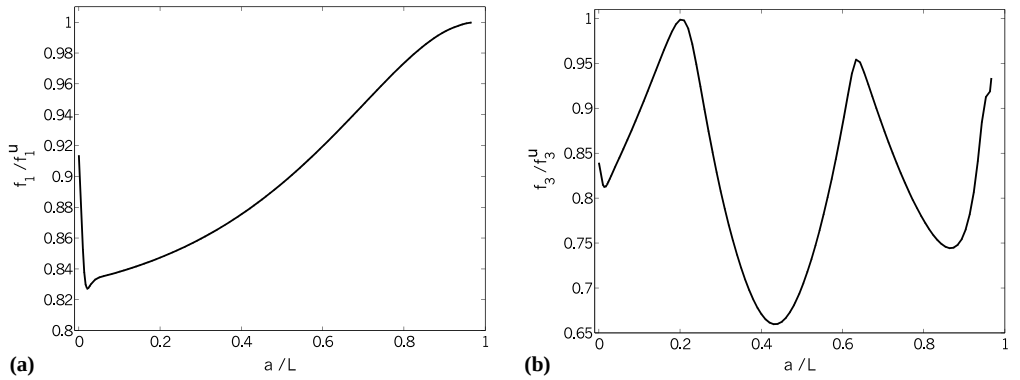

Fig. 4. Dependence of (a) the fundamental frequency and (b) the third natural frequency of the locally damaged sandwich cantilever in Fig. 3(a) on the location of the damage of length 10 mm along the span.

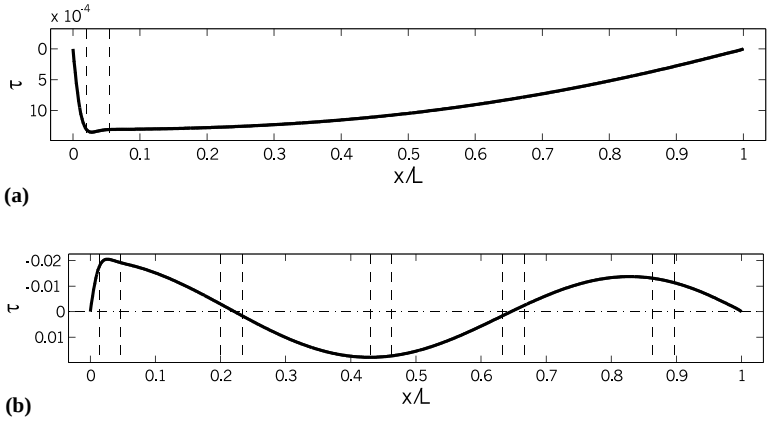

Fig. 5. Distribution of the shear stresses in the core along the span of the ordinary (undamaged) cantilever sandwich beam with the layout of Fig. 3(a) vibrating at: (a) fundamental frequency; (b) third natural frequency.

The dependence plotted in Fig. 4(a) exhibits global extremum points. The plot of Fig. 4(b), in addition, contains the local extremum points. Fig. 4(a) reveals that in the case of the fundamental frequency, the location of the local damage at the tip of the sandwich cantilever does not change the natural frequency. In addition, the lowest value for the fundamental frequency of the damaged beam, which is more than 17% lower than the fundamental frequency of the ordinary structure, is obtained in the vicinity of the supported edge.

A physical explanation of Fig. 4(a) is provided in Fig. 5(a), which shows the distribution of the shear stress in the core along the span of the ordinary sandwich cantilever, vibrating at the fundamental frequency. Note that the minimum value of the fundamental frequency in Fig. 4(a) is obtained when the local damage, acting similar to a shear hinge, wedges itself in the ordinary distribution of the shear stress near the point where it achieves the maximum value (see the dashed lines in Fig. 5(a)).

This also explains why the natural frequency is unaffected by the existence of a local damage at the tip of the sandwich beam, where the shear stress in the core vanishes. This insensitivity can be anticipated from considering the corresponding vibration mode pattern.

In the case of the third natural mode of the sandwich cantilever, the locations of the extremum points in the plot of Fig. 4(b) correspond to the location of the minima, maxima and zeros in Fig. 5(b). The lowest value of the third natural frequency of the damaged beam is obtained in the vicinity of the midspan ($x_d/L \sim 0.45$) and is 34% lower than the corresponding frequency of the ordinary beam.

Note that the core edge at the clamped end of the sandwich cantilever is assumed to be free of shear tractions (see Fig. 3(a)). As a result, the shear stress in the core achieves a maximum value at some distance from the supported edge (see Fig. 5(a)). This behavior can be predicted from the consistent higher-order approach, where the order of the governing partial differential equations matches the number of boundary conditions imposed on a sandwich beam.

4.2. Simply supported beam

Mode shapes of a locally damaged sandwich beam pinned at both upper and lower face sheets and with free core edges (Fig. 6(a)), are shown in Fig. 6(b). In this case, the small local midspan damage causes a ~25% reduction in the second and fourth natural frequencies (see Table 2). This reduction is in sharp contrast to the ordinary sandwich beam of the same layout (see Sokolinsky et al., 2002). Moreover, Fig. 6(b) shows that the third and fourth natural frequencies of the locally damaged sandwich beam are similar,

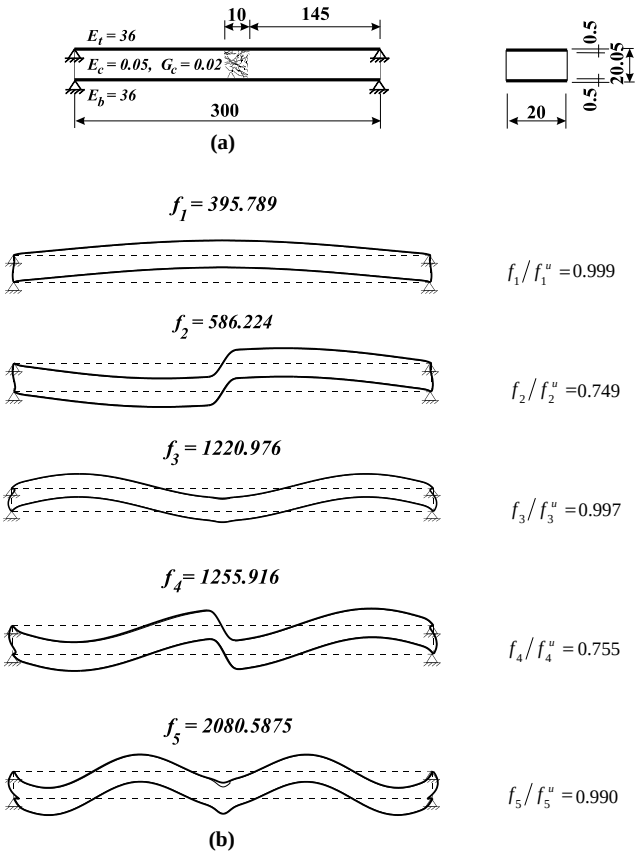

Fig. 6. "Simply supported" sandwich beam with local damage centered at midspan: (a) layout; (b) natural vibration modes and corresponding frequencies (Hertz) (dimensions in millimeters; moduli in gigapascal).

Table 2
Comparison of the natural frequencies of the "simply supported" sandwich beam

	Natural frequency (Hz)				
	1	2	3	4	5
Ordinary, f_n^u	395.9	783.1	1224.1	1662.7	2100.6
Damaged, f_n	395.8	586.2	1221.0	1255.9	2080.6
Difference, %	−0.03	−25.1	−0.3	−24.5	−0.9

unlike those of the ordinary sandwich beam. Notice also the localized deformation pattern in the fifth natural mode shape in Fig. 6(b), where the incompatibility in the vertical displacements of the upper face sheet and the core at the damaged region is clearly seen.

The dependence of the fundamental frequency, and of the second natural frequency of the "simply supported" sandwich beam in Fig. 6(a) at the site of the 10 mm local damage along the span is shown in Fig. 7(a) and (b), respectively. Fig. 7(a) shows that the lowest value of the fundamental frequency of the damaged beam 40% less than the corresponding frequency of the ordinary structure is obtained with the damage located at the beam edge, where the shear stress in the core reaches its maximum value. Furthermore, a local damage at the midspan, where the shear stress in the core vanishes, does not affect the value of the fundamental frequency. This is consistent with the explanations above concerning the cantilever sandwich beam.

Note that the region of the plot in Fig. 7(b) from the left side to the maximum point is qualitatively similar to the plot in Fig. 7(a) as expected from comparing the natural mode shapes corresponding to the two first natural frequencies of the "simply supported" sandwich beam in Fig. 6(b).

The effect of the length of a midspan damage on the fundamental and second natural frequencies of the "simply supported" sandwich beam of Fig. 6(a) appear in Fig. 8(a) and (b), respectively. The length of a midspan damage in Fig. 8 is varied from 1 to 25 mm. Fig. 8(a) shows that for the fundamental frequency, the 25-fold increase in the midspan damage length has a minor effect on the ratio of the natural frequency of the damaged sandwich beam to the corresponding frequency of the ordinary beam, although the relative rate of decrease in the frequency ratio significantly increases after the relative damage length becomes greater than 4% of the beam span. However, in the case of the second natural

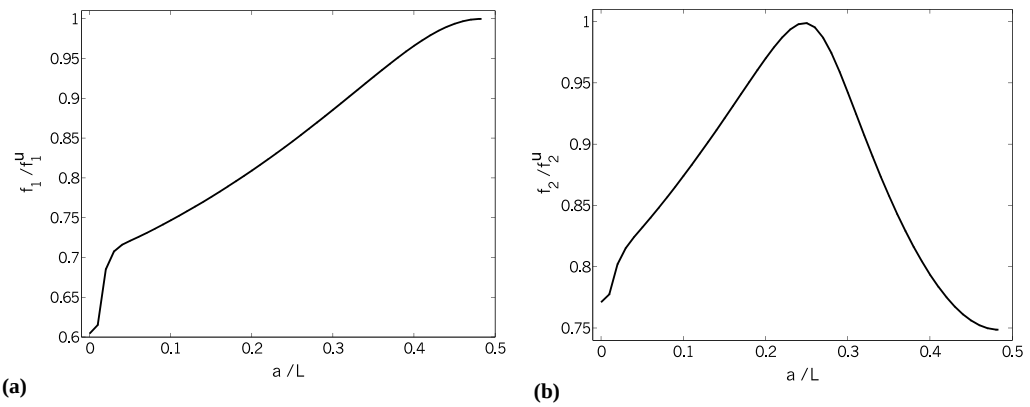

Fig. 7. Dependence of (a) the fundamental frequency and (b) the second natural frequency of the locally damaged "simply supported" sandwich beam in Fig. 6(a) on the location of the damage of length 10 mm along the span.

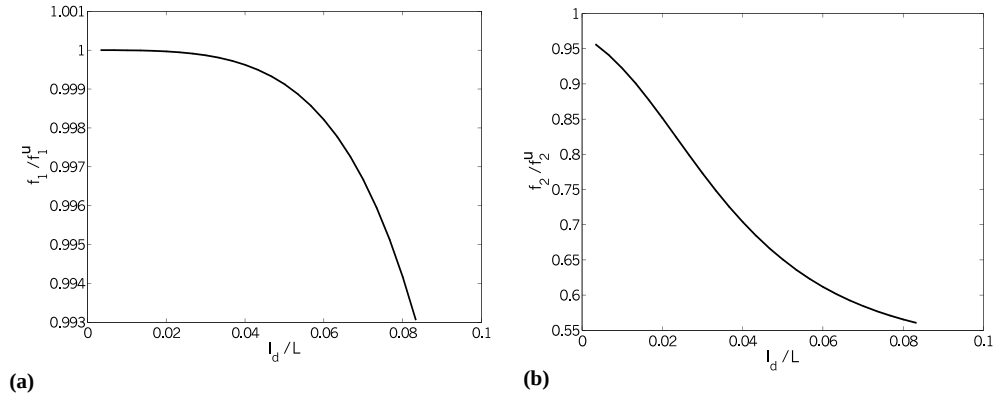

Fig. 8. Dependence of (a) the fundamental frequency and (b) the second natural frequency of the locally damaged "simply supported" sandwich beam in Fig. 6(a) on the length of a midspan damage.

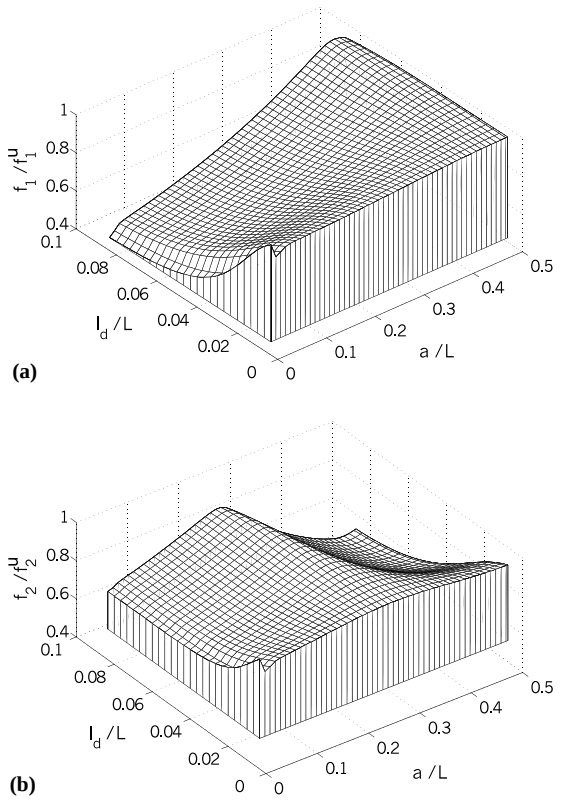

Fig. 9. Dependence of (a) the fundamental frequency and (b) the second natural frequency on the location and length of a damage in the span for the "simply supported" sandwich beam in Fig. 6(a).

frequency, the value of the frequency ratio drops by ~40% as the damage length increases from 1 mm up to 25 mm. Thus, the results in Fig. 8 reveal that the influence of the damage length on the specific natural

frequency of a soft-core sandwich beam depends on the *location* of the damage along the beam span. And, as shown previously, the effect of the location of a damage on the specific natural frequency depends on the distribution of the shear stress in the core corresponding to the vibration mode under consideration.

Additional simulations show that when the length of the local damage exceeds 8% of the beam span, the localized pattern in the midspan, similar to that of the fifth natural mode in Fig. 6(b), begins to develop in the symmetric vibration mode right at the fundamental frequency of the damaged sandwich beam.

The dependence of the first and second natural frequencies, on both, the location, and length of a local damage for the "simply supported" sandwich beam of Fig. 6(a) is shown in Fig. 9.

Finally, the effect of increasing face sheet thickness on the free vibration response of a locally damaged "simply supported" sandwich beam is considered (see Fig. 10). The thickness of each face sheet is increased from 0.2 to 5.6 mm, whereas the core volume and layout is otherwise the same as in Fig. 6(a). Fig. 10 shows that, in general, an increase in the face sheet thickness reduces the influence of a local damage on the vibration response of sandwich beams. However, the magnitude of the effect significantly depends on the mode shape. Namely, the effect on a specific natural frequency can be minor, as in the case of the fundamental mode in Fig. 10(a), and the effect can be dramatic, as in the case of the second natural mode in Fig. 10(b). As discussed previously, this behavior can be understood by considering the distribution of the shear stress in the core corresponding to the specific vibration mode.

Note that in the case of the fundamental frequency (see Fig. 10(a)), the dimensionless ratio f_1/f_1^u is very close to one (up to three decimal places). Therefore, the quantity $1 - f_1/f_1^u$ was used instead of the frequency ratio in order to increase the resolution of the plot.

The higher-order analysis presented here addresses the key physical aspects of the free vibration response of soft-core sandwich beams. As such, it can be used as an essential part in an identification method to determine the location and size of a local damage. An identification scheme, which utilizes the numerical results of the presented higher-order analysis and does not require an explicit functional form, is currently being developed (von Bremen et al., 2004).

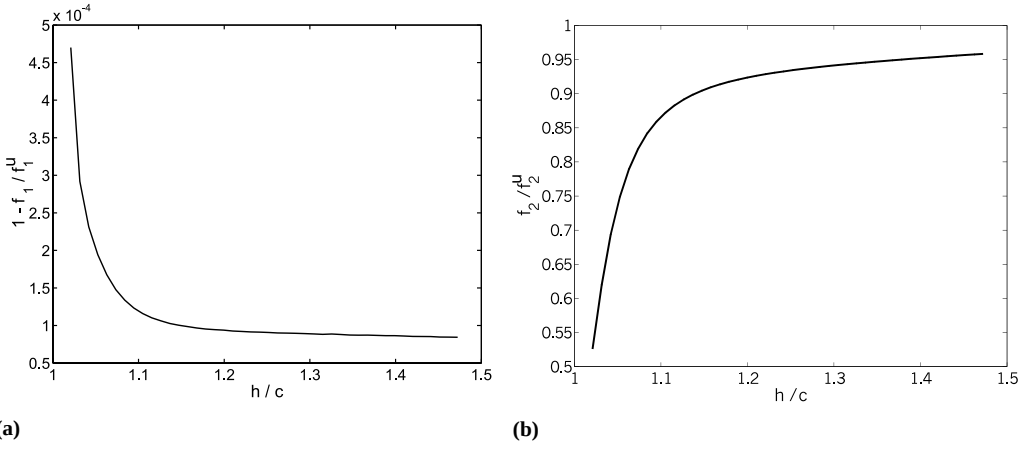

Fig. 10. Dependence of (a) the fundamental frequency and (b) the second natural frequency on sandwich thickness ratio for the locally damaged "simply supported" sandwich beam with the midspan damage of length 10 mm (Fig. 6(a)).

5. Confirmation of the higher-order analysis

The higher-order free vibration analysis of the delaminated sandwich beams with a locally damaged core was verified using the commercial finite element software ABAQUS (ABAQUS Users Manual, 2003). The finite element results of the natural frequencies and corresponding mode shapes of the cantilever (Fig. 3(a)) and simply supported (Fig. 6(a)) sandwich beam layouts were obtained and compared with those presented in the previous section. The Lanczos eigensolver of ABAQUS was used to compute the natural frequencies and corresponding mode shapes of the sandwich beam layouts under consideration.

Four-node two-dimensional plane-stress bilinear elements were used to model the sandwich beams. The parameters of the finite element meshes used here were chosen based on the mesh-sensitivity studies. In the case of the ordinary (undamaged) sandwich layouts, the face sheets were represented by 6 and the core by 39 elements through the thickness. Furthermore, there were approximately 2 elements per millimeter along the span of the beam. In the case of the damaged sandwich layouts, a substantially more condensed mesh was used near the damage region, with approximately three times more elements per millimeter along the span than for the undamaged region. The ordinary sandwich layouts were represented by a total of 32,844 elements, whereas in the case of the locally damaged sandwich layouts, a total of 30,287 elements were used. The number of elements used in the damaged case is less than that used for the ordinary case, because the core elements in the damage area were removed from the model to represent the locally damaged core. The boundary conditions of the cantilever sandwich beam (Fig. 3(a)) were modeled by constraining all the degrees of freedom of the nodes associated with the upper and lower face sheets and located at the left edge of the sandwich beam. For the simply supported layout (Fig. 6(a)), the translational degrees of freedom of the nodes associated with the mid-planes of the upper and lower face sheets and located at the left and right edges of the sandwich beam were constrained.

The natural frequencies of the ordinary and locally damaged cantilever and "simply supported" sandwich beams, which were calculated using ABAQUS, are compared with the higher-order results in Tables 3 and 4, respectively. And the corresponding vibration modes of the damaged cantilever and "simply supported" sandwich beams with a locally damaged core are shown in Figs. 11 and 12, respectively.

Tables 3 and 4 show that the natural frequencies of the ordinary and locally damaged sandwich beams, as calculated using ABAQUS, are in close agreement with the results of the higher-order analysis. The ABAQUS vibration modes in Figs. 11 and 12 are practically identical with those in Figs. 3 and 6, respectively. The small discrepancies between the finite element and higher-order calculations are attributed to the fact that the higher-order analysis neglects the longitudinal normal stresses in the core in the undamaged regions of a sandwich beam (see Section 2.1). On the other hand, the complexity of the finite element model made it more sensitive to the numerical errors, than it was the case for the much simpler higher-order model. The last comment is supported by the example of the "simply supported" sandwich

Table 3
ABAQUS vs. the higher-order results for the natural frequencies (Hz) of the cantilever sandwich beam

	Ordinary			Locally damaged		
	ABAQUS	Higher-order theory	Error, %	ABAQUS	Higher-order theory	Error, %
1	130.4	130.0	0.3	117.9	115.9	1.7
2	492.7	491.4	0.3	488.1	483.7	0.9
3	999.3	996.3	0.3	702.3	680.9	3.0
4	1470.8	1465.1	0.4	1301.3	1287.1	1.1
5	1941.2	1930.7	0.5	1743.5	1728.3	0.9

Table 4
ABAQUS vs. the higher-order results for the natural frequencies (Hz) of the "simply supported" sandwich beam

	Ordinary			Locally damaged		
	ABAQUS	Higher-order theory	Error, %	ABAQUS	Higher-order theory	Error, %
1	398.9	395.9	0.8	401.3	395.8	1.4
2	791.3	783.1	1.0	603.7	586.2	2.9
3	1235.9	1224.1	1.0	1240.6	1221.0	1.6
4	1676.8	1662.7	0.8	1282.4	1255.9	2.1
5	2116.5	2100.6	0.8	2116.7	2080.6	1.7

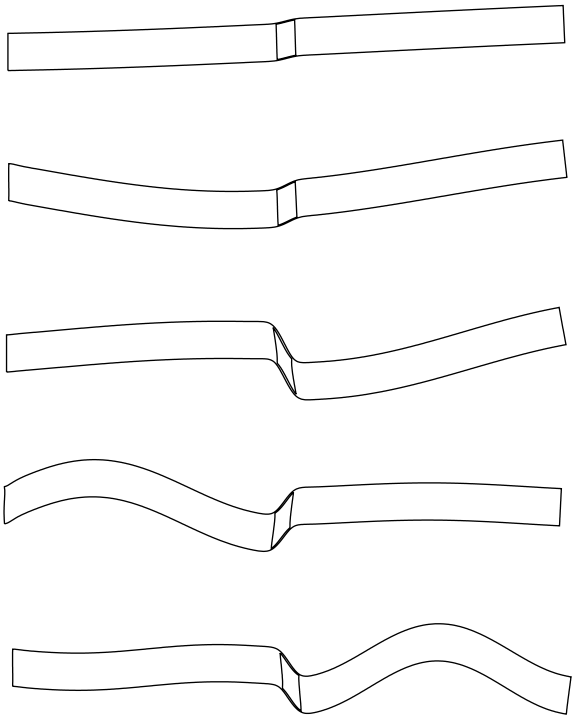

Fig. 11. ABAQUS results for the natural vibration modes of the locally damaged cantilever sandwich beam of Fig. 3(a).

beam, where the values of the first, third and fifth vibration modes were almost the same for the ordinary and damaged structures (see Table 2). In this case, ABAQUS produced slightly greater frequency values for the locally damaged beam than for the ordinary one. The higher-order calculations, however, consistently produced the lower values for the locally damaged structure as should be expected on physical grounds.

Note that the FEA results, which are comparable in accuracy with the present formulation, were achieved using the *two*-dimensional finite element model with a large number of degrees-of-freedom. On the other hand, the *one*-dimensional higher-order model required a relatively small (an order of magnitude less) number of degrees-of-freedom. Thus, using a finite element model in this case required significantly more intensive and costly numerical calculations.

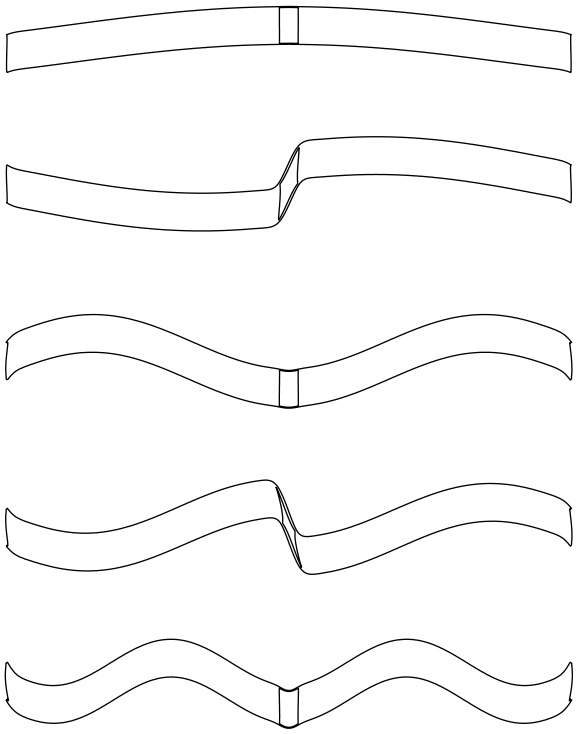

Fig. 12. ABAQUS results for the natural vibration modes of the locally damaged "simply supported" sandwich beam of Fig. 6(a).

6. Conclusions

The dynamical equations for free vibration response of sandwich beams with a locally damaged soft core have been derived using the higher-order theory approach, taking into account the nonlinear acceleration fields in the core. The present work shows that consideration of the nonlinear acceleration fields in the core is essential for analysis of the free vibration response of locally damaged sandwich beams, where the inertia loads exerted on the damaged structure are nonuniformly distributed along the span.

Numerical analysis based on the derived equations demonstrated that mode shapes of the sandwich beams with a locally damaged core *cannot*, in general, be described by a harmonic function of the longitudinal coordinate. Analysis of soft-core sandwich beam layouts, which are widely used in measurements of the natural frequencies of sandwich beams, revealed that small local damages in the core can cause a significant reduction in the natural frequencies and a dramatic change in the corresponding vibration modes of locally damaged sandwich beams.

The numerical study also revealed that a local damage in the core acts similar to a shear hinge. Locations of the damage at those portions of the beam span, where the shear stress in the core for the specific vibration mode reaches maximum absolute values, cause the greatest reduction in the corresponding natural frequency. Therefore, the influence of the damage length on the specific natural frequency of a soft-core sandwich beam depends on the *location* of the damage along the beam span.

An increase in the face sheet thickness reduces the influence of a local damage on the vibration response of sandwich beams, and the effect of this increase greatly depends on the mode shape and location of the local damage along the span of a sandwich beam.

The results of the higher-order formulation were verified through finite element analysis using the commercial software ABAQUS. The one-dimensional computational realization of the higher-order formulation required significantly fewer degrees-of-freedom than the two-dimensional FEA formulation.

The present work shows that vibration measurements may be used in the future to detect local damages in sandwich beams, a potentially useful capability for development of systems for nondestructive evaluation and material health monitoring.

Acknowledgements

The support of the Merwyn C. Gill Foundation is gratefully acknowledged. Special thanks are given to Dr. Zonghoon Lee for his help in preparation of the graphics. The authors of the manuscript thank the Editor-in-Chief and the reviewers for all their useful comments that have helped to significantly improve the paper.

References

ABAQUS Users Manual, 2003. Version 6.4, ABAQUS Inc., Pawtucket, Rhode Island, USA.

Cawley, P., Adams, R.D., 1979. A vibration technique for non-destructive testing of fiber composite structures. Journal of Composite Materials 13 (April), 161–175.

Frostig, Y., 1992. Behavior of delaminated sandwich beams with transversely flexible core-high order theory. Composite Structures 20 (1), 1–16.

Heal, K.M., Hansen, M.L., Rickard, K.M., 2000. Maple 6 Learning Guide. Waterloo Maple Inc., Waterloo, Ontario.

Hu, J.S., Hwu, C., 1995. Free vibration of delaminated composite sandwich beams. AIAA Journal 33 (10), 1911–1918.

Kim, H.-Y., Hwang, W., 2002. Effect of debonding on natural frequencies and frequency response functions of honeycomb sandwich beams. Composite Structures 55 (1), 51–62.

Kulkarni, S.V., Frederick, D., 1971. Frequency as a parameter in delamination problems—a preliminary investigation. Journal of Composite Materials 5 (January), 112–119.

Lanczos, C., 1997. The Variational Principles of Mechanics. Dover Publications, New York.

Lopez, R.J., 2001. Advanced Engineering Mathematics. Addison-Wesley, Boston.

Saad, Y., 1992. Numerical Methods for Large Eigenvalue Problems. Wiley, New York.

Shames, H.I., Dym, C.L., 1985. Energy and Finite Element Methods in Structural Mechanics. McGraw–Hill, New York.

Sokolinsky, V.S., Nutt, S.R., Frostig, Y., 2002. Boundary condition effects in free vibrations of higher-order soft sandwich beams. AIAA Journal 40 (6), 1220–1227.

Sokolinsky, V.S., Nutt, S.R., 2004. Consistent higher-order dynamic equations for soft-core sandwich beams. AIAA Journal 42 (2), 374–382.

Swanson, S.R., Kim, J., 2000. Comparison of a higher order theory for sandwich beams with finite element and elasticity analyses. Journal of Sandwich Structures and Materials 2 (1), 33–49.

The MathWorks. Reference Guide, Version 6, The MathWorks, Inc., Natick, MA, 2001.

Thomsen, O.T., Frostig, Y., 1997. Localized bending effects in sandwich panels: photoelastic investigation versus high-order theory. Composite Structures 37 (1), 97–108.

von Bremen, H.F., Sokolinsky, V.S., Nutt, S.R., 2004. Approach to identify debonding in soft-core sandwich beams. In: Proceedings of the 46th AIAA/ASME/ASCE/AHS/ASC Structures, Structural Dynamics, and Materials Conference, Palm Springs, California, April 19–22.